(19) N.-Å. Bergman, W. H. Saunders, Jr., and L. Melander, *Acta Chem. Scand.*, **26**, 1130 (1972), and references cited therein.
(20) H. Saitô, K. Nukada, T. Kobayashi, and Ken-ichi Morita, *J. Am. Chem. Soc.*, **89**, 6605 (1967).
(21) The difference between this temperature and that reported in the preliminary communication[6] is assumed to be due to the temperature measurement technique, which in the preliminary work involved a thermocouple in an empty, nonspinning 12 mm NMR tube. The same collapse temperatures as reported above were, however, obtained on several different samples on different occasions, and we thus feel confident about these values. In view of the comments of one of the referees on the validity of our present temperature measurement technique, we wish to point out that even if the *absolute* errors in the highest temperatures were as large as 5°, the *relative* error is certainly considerably smaller since all temperature measurements were made in exactly the same way. An absolute error as large as 5° has only a small effect on $\Delta G^{\ddagger}$ (of the order of 0.2 kcal/mol), but the parameter of interest is actually $\Delta\Delta G^{\ddagger}$, which will be affected by the relative error in the temperature measurements. The absolute error in temperature may reasonably be expected to be temperature dependent, thus introducing a source of systematic error in $\Delta H^{\ddagger}$, and $\Delta S^{\ddagger}$, but also here the "$\Delta\Delta$ quantities" are of most interest.
(22) The shifts on the experimental spectra could be estimated with the aid of the theoretical band shapes.
(23) S. Glasstone, K. J. Laidler, and H. Eyring, "The Theory of Rate Processes", McGraw-Hill, New York, N.Y., 1941, p 195 ff.
(24) R. W. Mitchell, J. C. Burr, Jr., and J. A. Merritt, *Spectrochim. Acta, Part A*, **23**, 195 (1967).
(25) (a) R. P. Bell, *Trans. Faraday Soc.*, **55**, 1 (1959); (b) "The Proton in Chemistry", 2nd ed, Chapman and Hall, London, 1973, p 270 ff.
(26) Drakenberg and Lehn[27] reported a difference of only −0.4 kcal/mol for $\Delta G^{\ddagger}$ (collapse temperature) in 1,2,2-trimethylaziridine on going from condensed ($(CH_3)_8Si_4O_4$ solution) to the gas phase. On the other hand, Harris and Spragg[26] found $\Delta G^{\ddagger}$ = 21.1 kcal/mol at 158°C for dimethylnitrosamine in the gas phase, compared with 23.3 kcal/mol in the liquid state.[29] These authors point out that "torsional barriers are generally lower in gases than in liquids",[28] but the difference between our results and those of Skaarup[7] cannot be explained on the basis of such an argument, in view of the agreement between our data and those of Nakanishi and Yamamoto.[6]
(27) T. Drakenberg and J. M. Lehn, *J. Chem. Soc., Perkin Trans. 2*, 532 (1972).
(28) R. K. Harris and R. A. Spragg, *Chem. Commun.*, 362 (1967).
(29) C. E. Looney, W. D. Phillips, and E. L. Reilly, *J. Am. Chem. Soc.*, **79**, 6136 (1957).
(30) The T_2 values used in the band shape analysis corresponded to effective line widths of ca. 2–3.5 Hz over the temperature range 10–155°C.
(31) E. F. Caldin and S. Mateo, *Chem. Commun.*, 854 (1973).
(32) For reviews of the tunnel effect, see: (a) E. F. Caldin, *Chem. Rev.*, **69**, 135 (1969); (b) M. D. Harmony, *Chem. Soc., Rev.*, **1**, 211 (1972).
(33) T. J. Bardos, C. Szantay, and C. K. Navada, *J. Am. Chem. Soc.*, **87**, 5796 (1965).

Role of Structural Flexibility in Conformational Calculations. Application to Acetylcholine and β-Methylacetylcholine[1]

Bruce R. Gelin and Martin Karplus*[2]

Contribution from the Department of Chemistry, Harvard University, Cambridge, Massachusetts 02138, and the Laboratoire de Chimie Théorique, Université de Paris VIII, Paris Ve, France. *Received March 7, 1975*

Abstract: The conformational properties of acetylcholine and β-methylacetylcholine are examined using an empirical energy function technique which permits energy minimization in the full conformational space of the molecule. Energy surfaces corresponding to rigid rotations about bonds are compared with those obtained by a complete energy minimization at each point. For the relatively uncrowded acetylcholine molecule, the differences between the two sets of calculations are minor. However, for β-methylacetylcholine, there is a significant reduction in the barrier heights and a large increase in the accessible conformational space. The geometric changes that relieve the large nonbonded repulsive contacts are analyzed and the results are compared with a series of INDO calculations based on the energy-minimized geometries. The sensitivity of conformational maps to the choice of starting geometry is also examined and an evaluation is given of the X-ray data used in previous conformational calculations.

I. Introduction

There have been many recent attempts to calculate conformational properties of pharmacologically interesting molecules.[3] Particular attention has focused on acetylcholine and related compounds which have served as the testing ground for a variety of theoretical methods.[4-12] Most of the conformational calculations have been carried out by selecting a geometry with fixed bond lengths and bond angles and systematically varying one or more dihedral angles of interest to produce an energy curve or surface. The methods used to obtain the conformational energy of the molecule as a function of the conformational parameters include empirical energy functions,[4b,5,6] Extended Hückel Theory (EHT),[4a,10] Intermediate Neglect of Differential Overlap (INDO),[8,9] Perturbative Configuration Interaction of Localized Orbitals (PCILO),[4c,11,12] and ab initio formulations of the STO-3G[13] and molecular fragment[7] types.

Typically the resulting energy surfaces show several low-energy valleys separated by barriers of various heights and surrounded by regions of such high energy as to preclude the molecule's existence in those areas. It has been assumed as a consequence that properties of the molecule, either in solution or when bound to a receptor site, may be understood by considering the low-energy regions. For a molecule like acetylcholine, where the maps found by most workers are rather nonrestrictive, such an assumption is possibly a reasonable one. However, for systems with a highly restrictive map, such as β-methylacetylcholine, a question must be raised concerning the possibility that "forbidden" regions might be made more accessible by relaxing some of the molecular constraints implicit in the calculations; that is, some of the strong steric repulsions that are involved in producing the high-energy regions may well be significantly reduced by including bond length and bond angle adjustment in the calculation. Production of a torsional angle conformational map with such "adiabatic" minimization of energy along all degrees of freedom is clearly a much larger task than that involved in the usual fixed-geometry maps. To investigate the importance of such effects without using excessive computer time, we have chosen an empirical energy-function

approach to the problem. This is done on the assumption that, although the quantitative results may be in error, the qualitative behavior is likely to be meaningful.

To illustrate the varying importance of structural flexibility, we examine in this paper the contrasting systems acetylcholine and β-methylacetylcholine. The unsubstituted -O-C_β-C_α-N^+ chain of the former is capable of relatively unhindered rotations about the -O-C- and -C-C- bonds, while the β-methyl substitution in the latter introduces considerable steric hindrance over large ranges of rotation for both bonds.

The empirical potential chosen for this work is that suggested by Lifson and Warshel.[14,15] It allows rapid minimization of the molecular energy with respect to all conformational variables, and optionally, the two dihedral angles of primary interest may be constrained to desired values while the energy is minimized with respect to all other conformational variables. The parameters for the potential function were taken in part from earlier work[14-16] and in part determined by fitting, with an iterative least-squares procedure,[14] to data available for small esters and amines. In the presence of significant steric repulsions, re-minimization of the conformational energy subject to constraint of the two dihedral angles is found to result in a considerable decrease of the energy. To check the validity of these results, a number of INDO energy calculations were carried out using the geometries located by the empirical energy function.

Section II reviews the empirical potential function and its present application. Section III defines the systems and conventions involved. Rigid-geometry maps and the importance of various energy contributions to them are described in section IV. Complete conformational flexibility is introduced in section V. Comparisons are made there between the variation of the empirical potential energy and the INDO energy. Section VI outlines the conclusions.

II. Empirical Potential Function

The approach on which the potential function is based has been described in detail elsewhere,[14-16] and we summarize only certain elements of its present application. The total molecular potential energy as a function of the Cartesian coordinates r is written

$$V(r) = \tfrac{1}{2}\sum_{\text{bonds}} K_b(b - b_0)^2 + \tfrac{1}{2}\sum_{\substack{\text{bonds}\\ \text{angles}}} [K_\theta(\theta - \theta_0)^2 + F(q - q_0)^2 + 2F'(q - q_0)] + \tfrac{1}{2}\sum_{\substack{\text{dihedral}\\ \text{angles}}} K_\phi[1 + \cos(n\phi - \delta)] + \tfrac{1}{2}\sum_{\text{nonbonded}} [As^{-12} - Bs^{-6} + e_i e_j s^{-1}] \quad (1)$$

The internal coordinates b, θ, and ϕ represent bond lengths, bond angles, and dihedral angles; q is the distance between atoms A and C of the bond angle A-B-C, and s is the distance between nonbonded atoms, i.e., those not bonded to each other or to a common atom. The corresponding empirical origins are the quantities b_0, θ_0, and q_0. Atomic charges e_i were obtained from INDO calculations, and a fixed set of nonbonded parameters A and B was used for all calculations. In the dihedral angle energy, n was either 2 or 3 and δ was 0 or 180°. The set of parameters thus includes K_b, K_θ, F, F', and K_ϕ for all the internal coordinate types in the molecules studied. Parameters not available from earlier work with the potential function, eq 1, were obtained by fitting computations of vibrational and conformational parameters to experimental data available for the molecules listed in Table I. Some modifications of previous parameters were required, and the entire final parameter set is listed in Table II.

Table I. Molecules Used for Parameter Refinement

Molecule	Type of data
Methyl formate	Vibrations[a,b]
	Conformation[c]
Methyl acetate	Vibrations[b]
	Conformation[d]
Ethyl acetate	Vibrations[e]
Larger esters	Skeletal vibrations (below 600 cm^{-1})[f]
Methylamine	Vibrations[g-i]
	Conformation[j]
Dimethylamine	Vibrations[g]
	Conformation[k]
Trimethylamine	Vibrations[g]
	Conformation[l]
Tetramethylammonium halides	Partial vibrations[m]
Ethylamine	Partial vibrations[h]

[a] H. Susi and J. R. Scherer, *Spectrochim. Acta, Part A*, **25**, 1243 (1969). [b] J. K. Wilmshurst, *J. Mol. Spectrosc.*, 1, 201 (1957). [c] R. F. Curl, *J. Chem. Phys.*, **30**, 1529 (1959). [d] J. M. O'Gorman, W. Shand, and V. Schomaker, *J. Am. Chem. Soc.*, **72**, 4222 (1950). [e] R. Nolin and R. N. Jones, *Can. J. Chem.*, **34**, 1392 (1956). [f] J. J. Lucier and F. F. Bentley, *Spectrochim. Acta*, **20**, 1 (1964). [g] G. Dellepiane and G. Zerbi, *J. Chem. Phys.*, **48**, 3573 (1968). [h] H. Wolff and H. Ludwig, *ibid.*, **56**, 5278 (1972). [i] J. R. Durig, S. F. Bush, and F. G. Baglin, *ibid.*, **49**, 2106 (1968). [j] D. R. Lide, *ibid.*, **27**, 343 (1957). [k] J. E. Wollrab and V. W. Laurie, *ibid.*, **48**, 5058 (1968). [l] J. E. Wollrab and V. W. Laurie, *ibid.*, **51**, 1580 (1969). [m] G. L. Bottger and A. L. Geddes, *Spectrochim. Acta*, **21**, 1701 (1965).

By employing the appropriate transformations between Cartesian and internal coordinates (and vice versa), the first and second Cartesian derivatives of eq 1 for an N-atom system

$$g_i = \frac{\partial V}{\partial x_i}, \quad G_{ij} = \frac{\partial^2 V}{\partial x_i \partial x_j}, \quad i, j = 1, 2, \ldots, 3N \quad (2)$$

can be obtained analytically and therefore can be computed extremely rapidly. Use of the first derivatives in the method of steepest descents and the second derivatives in a Newton-Raphson method allows minimization of the conformational energy. The resulting conformation typically has an RMS value of g_i around 0.1 kcal/(mol Å); that is, for any particular choice of potential function parameters in eq 1, a highly accurate converged minimum energy is obtained. For acetylcholine (26 atoms), 40 steepest descent steps followed by four Newton-Raphson minimizations requires about 15 sec (the computer used for all calculations was the IBM 360/91 computer at Columbia University).

A *rigid-geometry map* of the conformational energy as a function of two dihedral angles of interest is produced by leaving all bond lengths, bond angles, and other dihedral angles fixed, carrying out systematic variations (e.g., 10° rotations) of the two primary dihedral angles, and repeatedly evaluating the last two terms of eq 1, the first two terms remaining constant. For acetylcholine, the 1296 points of a 10° grid in two dihedral angles require about 45 sec of computer time.

To investigate the effects of structural flexibility on such a potential surface, the dihedral angles of interest are constrained to their grid values by addition of a large, steep potential acting only on these angles. The contribution from this term is not included in the molecular energy, but its contributions to the derivatives g_i and second derivatives G_{ij} serve to confine the dihedral angles to the chosen values,

Table II. Parameter List[a]

Bond type	Bond parameters (see eq 1) K_b	b_0
C–H	287.0	1.090
B–H	314.0	1.090
A–O	775.0	1.220
A–E	248.0	1.360
C–N	238.5	1.463
B–N	212.0	1.463
E–C	173.3	1.460
C–C	125.0	1.530
B–C	125.0	1.530
B–A	100.0	1.530

Angle type	Bond angle parameters (see eq 1)[b] K_θ	θ_0	F	F'	q_0
H–C–H	37.0	109.5	1.3	−0.10	1.779
C–C–H	30.0	109.5	47.6	−0.70	2.154
A–C–H	32.2	109.5	48.7	−0.60	2.084
N–C–H	32.5	109.5	57.5	0.10	2.099
E–C–H	28.2	109.5	41.8	−2.58	2.084
C–C–C	22.0	109.5	37.3	−1.55	2.498
C–C–N	33.2	109.4	45.5	0.10	2.450
C–C–E	27.0	109.4	42.0	−1.90	2.470
C–N–C	54.4	109.4	12.5	−1.84	2.400
C–A–O	29.1	119.0	35.3	0.98	2.357
C–A–E	40.7	117.0	40.1	0.77	2.448
E–A–O	144.6	123.2	88.5	1.00	2.270
A–E–C	42.5	109.4	43.8	0.90	2.320

Central bond	Dihedral angle parameters (see eq 1) K_ϕ	n	δ
C–C[c]	0.6	3	0
B–C[d,e]	0.2	3	0
C–N[f]	0.3	3	0
B–N[d]	0.3	3	0
A–E[g]	5.782	2	180
E–C[c]	0.186	3	0
B–A[d]	0.140	3	0
Carbonyl[c] out-of-plane	9.5	2	180

Pair	Nonbonded parameters (see eq 1)[h] A	B
H···H	1842	5.75
O···H	13969	42.4
N···H	15303	40.5
N···O	96576	298.3
C···H	29825	49.0
C···O	224917	360.0
C···N	238728	339.2
C···C	426454	391.8

[a] Energy in kcal/mol; distances in Å; angles in deg except that radians are used in computations involving K_θ. The parameters are defined in terms of the following atom types: H, any hydrogen; O, carbonyl oxygen; N, tetrahedral nitrogen; C, methylene carbon ($-CH_2-$); A, carbonyl carbon; B, methyl carbon ($-CH_3$); E, ester oxygen. [b] B and C are treated as equivalent. [c] Force constant applied once to the single heavy-atom definition of torsion. [d] Force constant applied three times, once for each of three terminal hydrogens. [e] Occurs only in β-methylacetylcholine; defined with respect to ester oxygen. [f] Force constant applied three times once for each possible heavy-atom definition of torsion. [g] Force constant applied twice, once for each possible heavy-atom definition of torsion. [h] E and O are treated as equivalent; A, B, and C are treated as equivalent.

while all other dihedral angles, bonds, and bond angles are free to vary as energy minimization is carried out. Repeated calculations of this type produce a *flexible-geometry map*. Thirty steepest descents and three Newton-Raphsons were used to find the minimum energy geometry for each set of

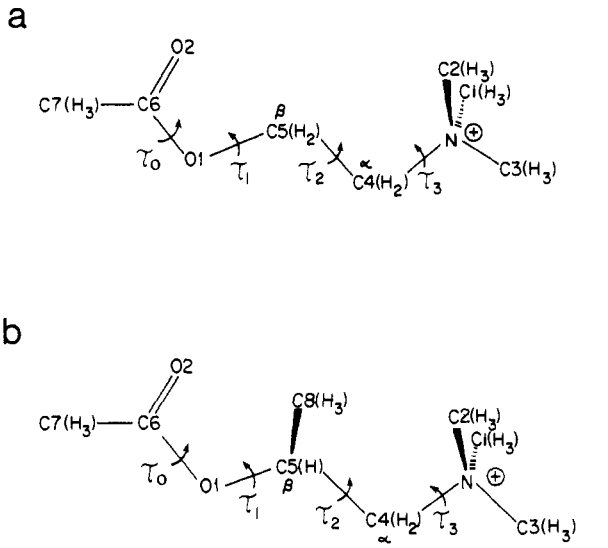

Figure 1. Structural diagrams of (a) acetylcholine and (b) β-methylacetylcholine, showing atom and dihedral-angle labels.

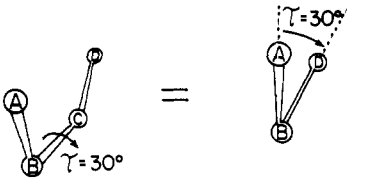

Figure 2. Definition of dihedral angle.

dihedral angles; when very large steric repulsions are present in the starting geometry, this procedure does not achieve the small gradient mentioned above, but does lead to a great reduction of the repulsive term. With a 20° mesh in two dihedral angles, acetylcholine (requiring only half the surface, because of molecular symmetry) could be mapped with about 35 min of computer time; β-methylacetylcholine, which has three more atoms and no symmetry, required about 70 min.

In all the surface calculations, both the total energy and the separate contributions corresponding to each of the sums in eq 1 were stored at every point of the surface. This allows comparisons of the various energy contributions and their roles in relieving internal steric hindrance. Selected final geometries obtained during the flexible mapping were used for energy calculation with an INDO program.

Froimowitz and Gans[6] have noted that empirical potential energy calculations are about four orders of magnitude faster than INDO and related semiempirical methods for producing rigid-geometry maps. We find that the present method can produce a *flexible*-geometry map in about the same time as INDO requires for a *rigid* map. Thus, it is clear that an empirical potential is the only one possible, in terms of computer time, for studies of structural flexibility.

III. Definitions and Conventions

Acetylcholine and β-methylacetylcholine are diagrammed in Figures 1a and 1b, with standard atom and dihedral-angle labeling. The two dihedral angles of primary interest are $\tau_1 = \tau$(C6-O1-C5-C4) and $\tau_2 = \tau$(O1-C5-C4-N). The sense of the dihedral angles, Figure 2, is the standard IUPAC definition such that a dihedral angle has the same value when viewed from either end, and the eclipsed cis conformation corresponds to 0°. The carbonyl out-of-plane distortion is measured as the angle between two planes, the first defined by atoms C7, O2, and

C6, and the other by O2, C6, O1 (see Figure 1); for a planar ester group, this angle is 180°.

We plot the potential surfaces with τ_1 on the x axis and τ_2 on the y axis. Accordingly we write a pair of values for τ_1 and τ_2 as if they were an (x,y) coordinate pair. The crystal structure of acetylcholine bromide thus has (τ_1,τ_2) = (79,77) while for the chloride (τ_1,τ_2) = (−167,85) = (193,85). This differs from an alternative convention in which τ_2 is written first and the pair is enclosed in brackets or braces, e.g., $\{\tau_2,\tau_1\}$. However, we find the coordinate pair convention more convenient.

IV. Rigid-Geometry Results

For acetylcholine and its analogs there exist a large number of rigid-geometry calculations.[4-13] Although we do not wish to make detailed comparisons with each of them, it is worthwhile to use the great speed of the present mapping potential to study the origins of some discrepancies which exist in the literature.

A. Choice of Rigid Geometry. There are three common ways to obtain a set of atomic coordinates to specify a molecular geometry: (1) X-ray crystallographic studies; (2) model building using idealized or accepted values of bond lengths, bond angles, and dihedral angles; and (3) energy minimization of some potential function such as eq 1, beginning with coordinates from (1) or (2) and arriving at the nearest local minimum.

The X-ray geometries of acetylcholine and related molecules show considerable variation in corresponding internal coordinates. Figures 3a-c show the X-ray geometrical parameters for acetylcholine bromide,[17] acetylcholine chloride,[18] and β-methylacetylcholine iodide,[19] with the corresponding empirical potential local minima. In the three "experimental" structures, the C4-N bond length, for example, varies from 1.49 to 1.59 Å, and C5-C4 from 1.43 to 1.52 Å. The large differences in bond lengths and bond angles between the two structures of acetylcholine are not borne out by the energy minimizations. There is clearly a question concerning the significance of these differences, which is commented on in the Appendix.

B. Rigid Geometry Surfaces. For both the relatively unhindered acetylcholine and sterically crowded β-methylacetylcholine, the rigid-geometry surfaces produced by previous authors have similar sizes and shapes of conformationally allowed regions, and the positions of local minima are in overall agreement. However, the particulars of the well depths, barrier heights, and relative ordering of the minima are found to be quite variable. These differences could arise from the form of the potential function method, the choice of geometry, or both.

Froimowitz and Gans[6] have analyzed their rigid-geometry surface, which includes electrostatic and nonbonded contributions, and have also discussed the nature of nonbonded forces in an INDO treatment. Their results indicate why the empirical energy-function method gives shallower wells, and why INDO local minima are tightly packed against very steep repulsive potential barriers.

The nonbonded and electrostatic contributions to the empirical potential, eq 1, were mapped using the acetylcholine bromide geometry and are displayed in Figures 4a and 4b. Although the present parameterization is somewhat different, the results are very similar to Figures 3 and 4 of ref 6. Equation 1 includes an additional torsional contribution, shown in Figure 4c, whose effect is to raise the local minima in proportion to their distance from the torsional minima at 60, 180, and 300°. The sum of nonbonded and electrostatic terms produces Figure 5a; addition of the torsional contribution produces Figure 5b and shows how inclusion of the

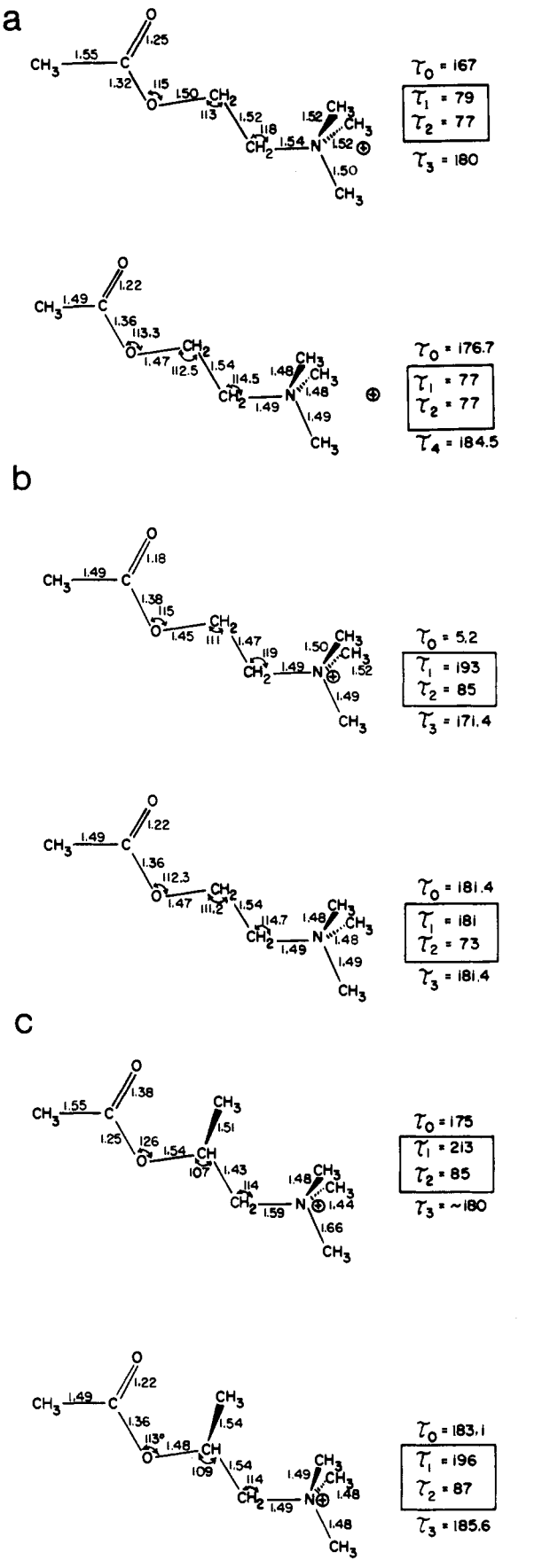

Figure 3. Comparison of X-ray crystal geometries with corresponding empirical energy-function local minima; bond lengths in ångströms, bond angles in degrees, and dihedral angles in degrees at right of each figure. In each pair upper figure shows experimental geometry: (a) acetycholine bromide (see ref 17); (b) acetylcholine chloride (see ref 18); (c) β-methylacetylcholine iodide (see ref 19).

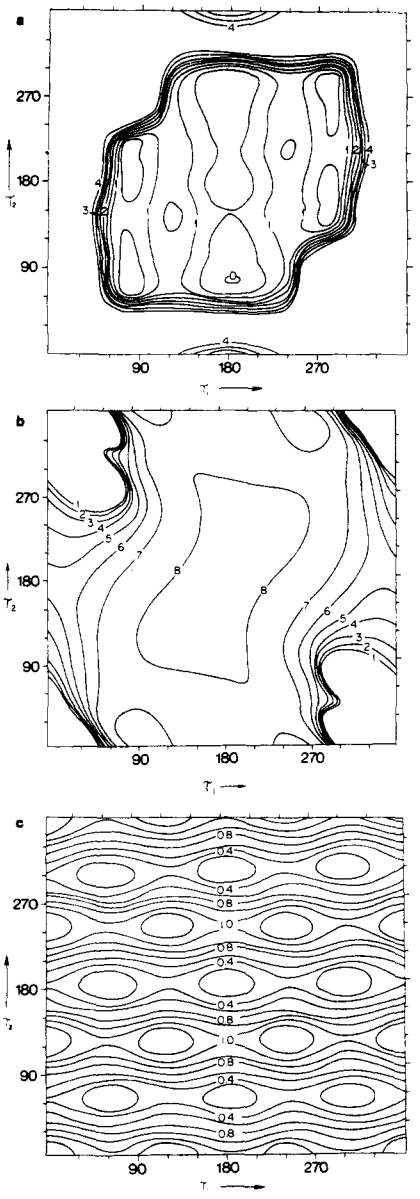

Figure 4. Empirical energy maps for rigid acetylcholine bromide crystal geometry; contour labels in kcal/mol: (a) nonbonded contribution; (b) electrostatic contribution; (c) torsional contribution.

torsional potential results in a surface with somewhat larger barriers but with all minima falling within about 1.5 kcal/mol of each other. This result is somewhat similar to those of ref 4b and 5, where a torsional potential is included.

The empirical energy function methods thus lead to a flat surface with closely spaced local minima, while the INDO, PCILO, and ab initio formulations predict energy differences of several kilocalories per mole for the local minima. Two recent NMR results[20,21] suggest a very close spacing (less than 1.0 to 1.5 kcal/mol) of two conformations, one much like the chloride crystal at about (180,70) and the other a fully extended form (180,180). This is in agreement with the energy function results. However, it must be cautioned that solvent perturbations are not included explicitly in any of the calculations, so that a direct comparison with solution data may not be valid.[22] Also, as pointed out in the introduction, molecular calculations of the type considered here may well be quantitatively in error so that differences of 1 or 2 kcal are not likely to be significant.

In order to examine the role of geometrical input, the mapping procedure was repeated for the energy-minimized geometry from eq 1, and the chloride crystal geometry (modified to have a symmetrical onium group). The contributions are similar to those shown in Figure 4, and we present only the total energy maps (nonbonded plus electrostatic plus torsional) in Figures 5c and 5d. It can be seen that the general features of the surfaces are similar in all calculations, but that details of barrier heights and relative minima are more sensitive to geometrical input. In their PCILO study, Pullman et al.[11] noted that use of the chloride crystal geometry produces a lower minimum at approximately (180,70), in the neighborhood of that found in the crystal. They argue that use of a given geometrical input tends to favor the conformation associated with it, relative to the other minima. Such a correlation would appear likely if the geometric distortions (the changes in bond lengths and bond angles) observed in the crystal were valid; unfortunately, the available data may not be sufficiently accurate (see Appendix). In our maps, the chloride geometry does produce its corresponding minimum at a lower energy, but all other local minima are lowered by about the same amount. Similar results are found with an energy-minimized geometry (the minimization was carried out at (180,180)) in which the internal coordinates more closely resemble those of the chloride crystal geometry. This may indicate that some of the internal coordinate distortions in the bromide geometry are more questionable than those of the chloride. For both chloride crystal and energy-minimized geometrical input, the minimum at (180,70) is lower than that at (80,80), and the maps are flatter overall.

For β-methylacetylcholine, the rigid geometry map is almost completely dominated by nonbonded forces, most of the surface being sterically forbidden. Figures 6a and 6b show the total-energy surfaces obtained from the iodide crystal geometry and from the eq 1 energy-minimized geometry. The two maps have similar minima and allowed regions, but have large differences in the energies of the secondary minima and in the height of the barrier in the region $\tau_1 \simeq 100$ to 150°, $\tau_2 \simeq 70$ to 100°. In this region, the energy-minimized geometry leads to an enormous barrier whereas the iodide crystal geometry has a barrier of only about 10 kcal. The origin of this barrier is nonbonded repulsion between the β-methyl group and the carbonyl oxygen; its variation is explained by the larger experimental values for the C6-O1-C5 bond angle (126°) and the O1-C5 bond length (1.54 Å), which allow the methyl group to pass by the carbonyl oxygen without excessively close contacts. While these two geometrical parameters seem abnormally large, it is interesting to note that flexible-geometry studies (vide infra) give a barrier height very similar to that in the experimental-geometry map and substantiate the opening of the bond angle C6-O1-C5. The empirical rigid-geometry map suggests that energy minimization has optimized the structure for the global minimum at (196,87) to the detriment of the rest of the surface.

In view of the dependence of rigid-geometry maps on geometrical input, it appears that it is not sufficient to study the conformational properties of an internally hindered molecule on the basis of a single rigid map. Some more complete study is needed, such as multiple rigid maps using various starting geometries, or, as is done below, inclusion of structural flexibility in the mapping procedure.

V. Flexible-Geometry Results

Since the potential energy of a molecule like acetylcholine depends on geometric parameters other than the two dihedral angles, it is essential to determine the effect of all degrees of freedom. The visualization of the $3N$-dimensional energy surface for an N-atom system in terms of two dihedral angles has been described in section II.

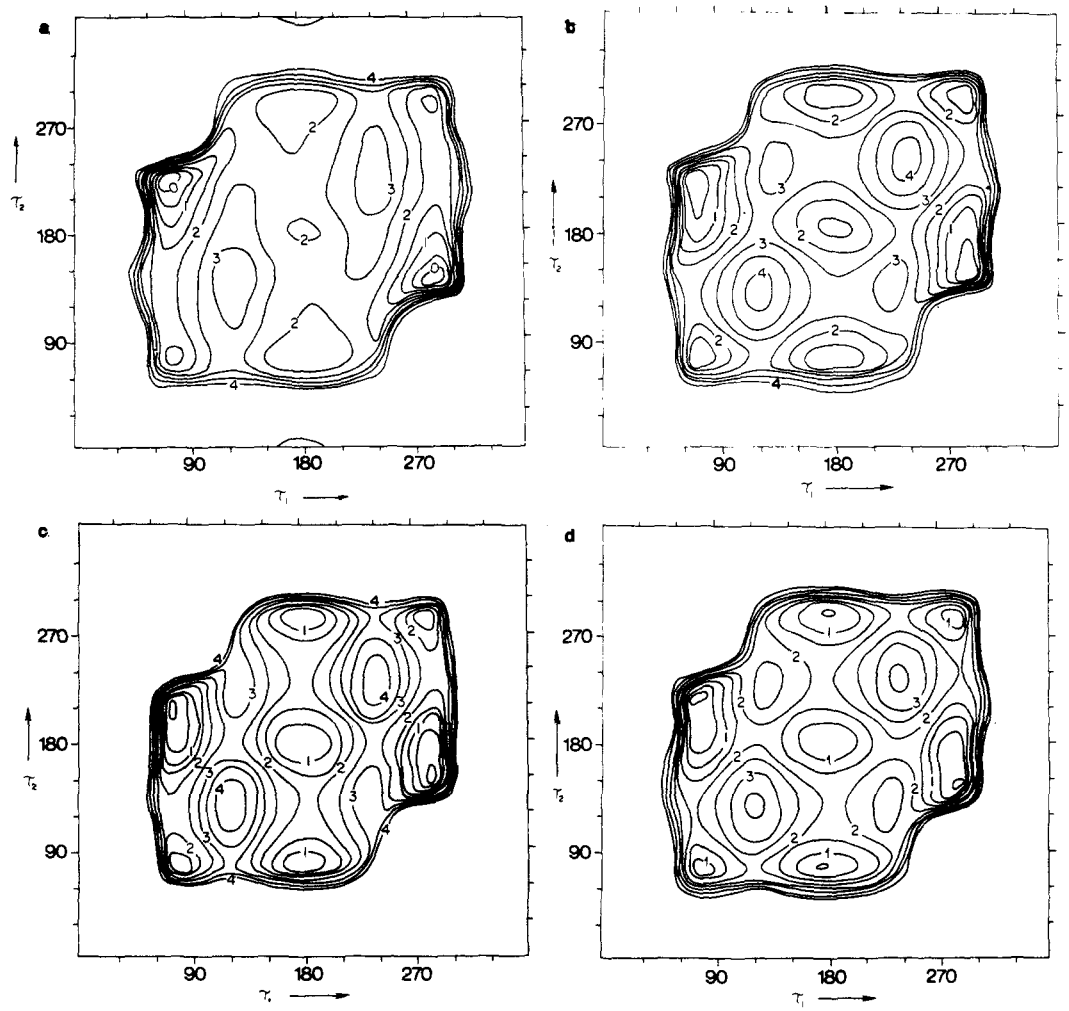

Figure 5. Empirical energy maps for acetylcholine; energy contours in kcal/mol: (a) Bromide crystal geometry: sum of nonbonded and electrostatic terms. (b) Bromide crystal geometry: sum of nonbonded, electrostatic, and torsional terms (total empirical energy for rigid geometry). (c) Same as (b), but with energy-minimized geometry $(\tau_1,\tau_2) = (180,180)$. (d) Same as (b), but with chloride crystal geometry.

Increased geometric flexibility allows a molecule to find ways of relaxing nonbonded repulsions, particularly when steric crowding is important. In that case, the energy cost associated with a rigid twist of a dihedral angle may become as large as that needed to open a bond angle or distort some other degree of freedom customarily treated as fixed. In this section we report the results of including structural flexibility in the mapping calculations for acetylcholine and β-methylacetylcholine and discuss the relationship of these results to those obtained assuming a rigid geometry.

A. Acetylcholine. The flat central portion of all the rigid acetylcholine maps indicates an essentially unhindered region of conformational space for the O-C-C-N^+ chain. Addition of further conformational freedom therefore does not significantly alter this part of the map, although some broadening of the minima is seen in Figure 7, which compares rigid and flexible maps.

The blank periphery of the rigid maps, which corresponds to regions with considerable steric hindrance, is most affected by the flexible geometry. As rotation of the dihedral angles of interest brings parts of the molecule close together and their steric repulsion increases, energy minimization can lead to a significant "relaxation" of the molecule. In the present calculations, as well as in related work on hindered polyenes,[16] bond angle distortions are found to be most important. Of importance also are ester group deviations from planarity, which are related to the effect found in studies of the peptide bond by Winkler and Dunitz.[23]

Two examples of relaxation of steric hindrance through structural distortion of acetylcholine are presented in Tables III and IV. In both of these cases the steric hindrance arises from the short distance between the ester group and the $-N(CH_3)_3$ group. Table III shows the skeletal bond angles and dihedral angles whose distortions decrease the nonbonded interactions. Comparison of the bond angles with the values in Figure 3 shows distortions of up to 10°. At $\tau_1 = 320°$, the ester bond τ_0 rotates 20° from planarity, corresponding to an energy of about 2.7 kcal/mol with the present energy functions. Also, methyl hydrogens are removed from close contacts by rotations of up to 30° about the bonds N-Ci (not listed in Table III).

The barrier involved in the case of Table IV is illustrated in Figure 8, which shows slices of the (τ_1,τ_2) surfaces for $\tau_1 = 180$. This figure shows how small the differences are between rigid and flexible maps in the central region, and how the barriers to internal rotation are reduced. The curves show variations of energy with τ_2 and should be compared with Figure 4 of ref 7, which shows the corresponding EHT, PCILO, INDO, and molecular fragment ab initio rigid-geometry results.

Figure 8, which is a vertical slice along Figures 7a and 7b, also shows that the minimum at approximately $(\tau_1,\tau_2) = (180,360)$, which is found in both the present and other rigid-geometry maps, is actually a saddle point in the flexible study. The "articulation" of the onium group with the carbonyl is illustrated by the angles (C5-C4-N-Ci) in

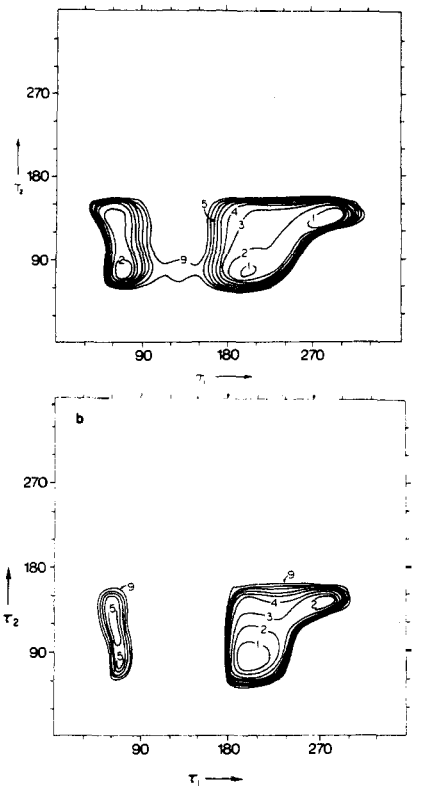

Figure 6. Total empirical energy maps for β-methylacetylcholine; contour labels in kcal/mol: (a) iodide crystal geometry; (b) energy-minimized geometry for (τ_1,τ_2) = (196,87).

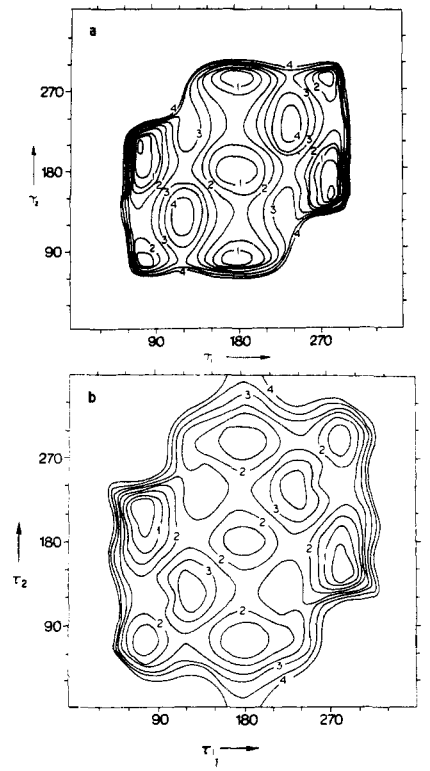

Figure 7. Comparison of rigid- and flexible-geometry maps for acetylcholine; contour labels in kcal/mol: (a) rigid energy-minimized geometry; (b) flexible geometry.

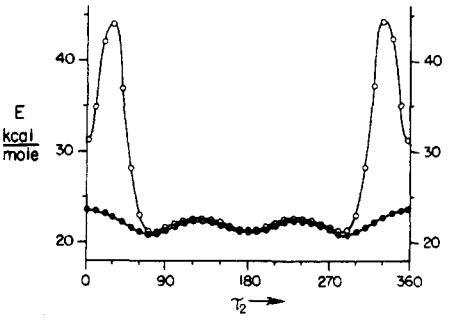

Figure 8. Empirical energy of acetylcholine as a function of τ_2, with τ_1 fixed at 180°: (○) rigid geometry; (●) flexible geometry.

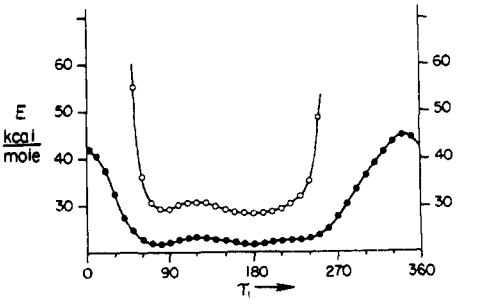

Figure 9. Empirical energy of acetylcholine as a function of τ_1, with τ_2 fixed at 50°: (○) rigid geometry; (●) flexible geometry.

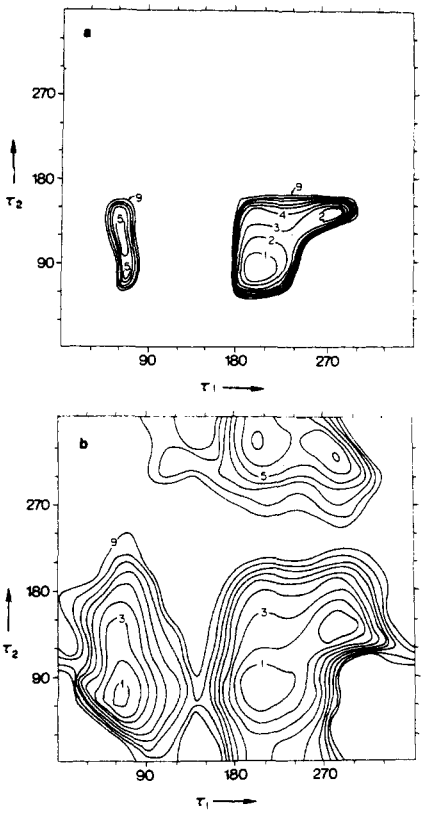

Figure 10. Comparison of rigid- and flexible-geometry maps for β-methylacetylcholine; contour labels in kcal/mol: (a) rigid energy-minimized geometry; (b) flexible geometry.

Table IV; they increase from the normal values of 60, 180, and 300 as the onium approaches the carbonyl, then change to smaller values as the onium passes the carbonyl.

Figure 9 examines a portion of the surface closer to the blank periphery of the rigid map and shows the effects of structural flexibility more vividly. This figure displays energy variation with τ_1, for τ_2 = 50°; the rigid-geometry bar-

Table III. Acetylcholine Flexible Geometry (τ_1 = 260 to 360°, τ_2 = 100°)

τ_1	τ_2	C6–O1–C5	O1–C5–C4	C5–C4–N	τ_0	Carbonyl out-of-plane	τ(C5–C4–N–C_i) i = 1	i = 2	i = 3
260	100	116.4	113.1	118.2	179.5	180.1	60	177	296
280	100	119.3	116.5	120.1	176.1	182.5	60	176	295
300	100	121.8	119.0	122.9	167.0	182.5	57	174	293
320	100	123.4	121.3	123.1	160.1	179.7	56	173	291
340	100	123.3	123.2	114.4	187.1	176.3	62	179	299
360	100	122.8	122.6	115.1	182.5	176.1	58	178	296

Table IV. Acetylcholine Flexible Geometry (τ_1 = 180°, τ_2 = 360 ± 60°)[a]

τ_1	τ_2	C6–O1–C5	O1–C5–C4	C5–C4–N	τ(C5–C4–N–C_i) i = 1	i = 2	i = 3
180	300	112.5	112.2	115.5	61	180	298
180	320	112.6	113.6	116.3	65	184	302
180	340	112.5	114.6	116.9	68	186	304
180	360	112.4	115.3	117.5	62	180	298
180	20	112.5	114.7	116.9	57	175	293
180	40	112.6	113.6	116.3	58	176	295
180	60	112.5	112.2	115.5	61	180	299

[a] Slight deviations from symmetry (or antisymmetry) about (τ_1, τ_2) = (180, 360) result from incomplete energy minimization in the flexible-geometry map (see section II).

Table V. β-Methylacetylcholine (τ_1 = 60 to 200°, τ_2 = 80°)

τ_1	τ_2	C6–O1–C5	O1–C5–C8	τ_0	Carbonyl out-of-plane	τ(O1–C5–C8–H_i) i = 1	i = 2	i = 3
60	80	116.9	110.7	178.5	180.2	69	189	309
80	80	116.5	114.4	175.2	182.3	77	198	317
100	80	118.9	117.4	175.4	182.7	75	196	316
120	80	120.9	119.1	175.9	181.4	68	189	309
140	80	122.8	120.5	182.0	178.1	87	210	329
160	80	118.1	115.7	185.4	176.6	87	207	327
180	80	114.2	111.9	182.8	178.5	84	204	324
200	80	113.1	109.9	181.3	179.4	82	202	323

riers rise to hundreds of kilocalories at the ends of the slice, while the flexible-geometry barrier is only about 20 kcal. This figure should be compared with Figure 3 of ref 7, which plots the INDO, PCILO, and molecular fragment energies.

B. β-Methylacetylcholine. Due to its overall greater steric hindrance, β-methylacetylcholine is a more striking example of the effects of structural flexibility. This can be seen through the comparison in Figure 10 of rigid and flexible maps; separate contributions to the flexible map are shown in Figures 11a through 11d.

The electrostatic map, Figure 11a, is similar to that obtained with rigid geometries and has a high central plateau with lower energies at the corners of the map where oppositely charged groups may approach closely. The similarity of rigid and flexible maps is due to the slowly varying $1/r$ dependence of electrostatic energy and the fact that changes in atom positions upon energy minimization are not large.

The nonbonded map, Figure 11b, is remarkably flat in view of its dominance in the rigid case (Figure 6b), where contributions of hundreds of kilocalories were present over much of the map. The extreme steepness of the repulsive term of the Lennard-Jones potential, which varies as $1/r^{12}$, means that small changes in atomic position can bring about large decreases in energy and leave the residual contributions comparable to those of other terms of the potential in eq 1.

The torsional surface, Figure 11c, is quite flat, retaining suggestions of periodic minima every 120° for both τ_1 and τ_2. The higher corners of the map now include contributions from the ester dihedral angle τ_0, out-of-plane bending of the carbonyl group, and other dihedral angles as noted in Tables III and IV.

Bond stretching contributes minimally to the results and is not shown. Except at the corners of the map, bond length distortion amounts to less than 1 kcal/mol, the large bond force constants K_b in eq 1 making it easier to absorb strain energy in other internal coordinates.

It is seen from Figure 11d that bond angle distortion makes up a dominant component of the total energy and parallels it to a great extent over the whole surface. The bond angle contribution is largest in the regions of the surface where the rigid map showed the largest nonbonded steric repulsion, and thus is responsible for relieving it.

Table V shows how internal coordinates of β-methylacetylcholine deviate from their normal values in order to relieve the large barrier to rotation for τ_1 = 60 to 200° with τ_2 fixed at 80°. The barrier arises from approach of the carbonyl oxygen and the β-methyl group (carbon C8 and its three hydrogens). At τ_2 = 80°, the $-N(CH_3)_3$ group is almost trans to C8. Along the path, the bond angle C6–O1–C5 opens to nearly 123°, and O1–C5–C8 to nearly 121°, much closer to the iodide crystal structural parameters than the energy-minimized geometry (see Figure 3c). Also the ester bond τ_0 and carbonyl out-of-plane dihedral angles show distinct jumps when the methyl group passes the carbonyl. A nearby slice of the potential surface, for τ_2 = 60°, is shown in Figure 12. Results of three calculations using the empirical potential are shown, all with respect to the

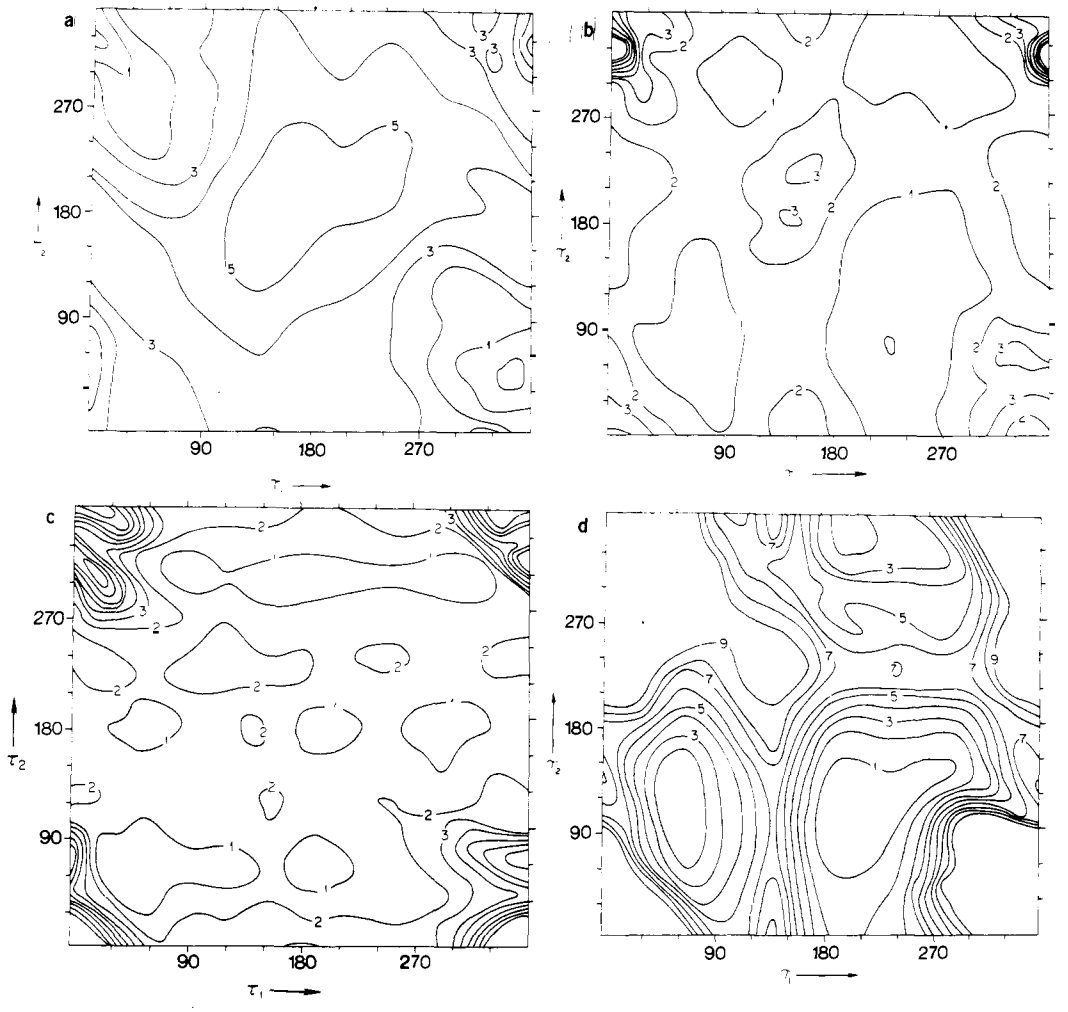

Figure 11. Contributions to flexible-geometry map for β-methylacetylcholine; contour labels in kcal/mol: (a) electrostatic; (b) nonbonded; (c) torsional; (d) bond angle.

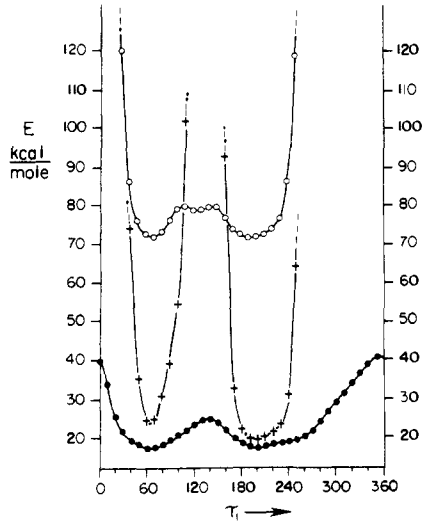

Figure 12. Effect of geometry on empirical energy of β-methylacetylcholine as a function of τ_1, with τ_2 fixed at 60°: (O) rigid iodide crystal geometry; (+) rigid energy-minimized geometry; (●) flexible geometry.

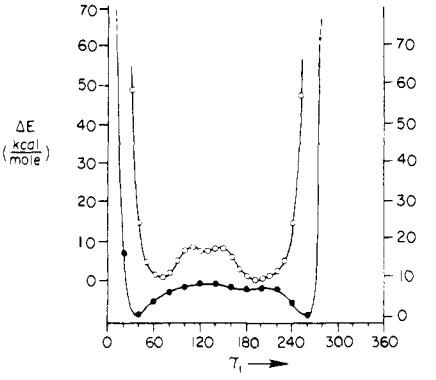

Figure 13. Comparison of empirical and INDO energies of β-methylacetylcholine as a function of τ_1, with τ_2 fixed at 60°, using rigid energy-minimized geometry: (O) empirical energy (left-hand scale); (●) INDO energy (right-hand scale).

same zero of energy: iodide crystal rigid geometry highest, because of the nonideal values of many internal coordinates; energy-minimized rigid geometry lower at the minima, but having a much larger barrier; and the flexible-geometry results lowest, with a maximum barrier (at $\tau_1 = 350°$) of only 43 kcal/mol. It is important that all three calculations produce local minima in very similar positions. Even for crowded, internally hindered systems, it seems that a rigid-mapping procedure can give a good estimate of the location of the minima.

As a partial check of the significance of the present approach, we have calculated empirical potential energies and INDO energies for two slices, using the same geometries for both calculations. The results are shown in Figures 13 and

Table VI. X-Ray Structural Parameters of Cholinergic Molecules

Molecule	C6–O1	O1–C5	C5–C4	C4–N	C6–O1–C5	O1–C5–C4	C5–C4–N
Acetylcholine bromide[a]	1.32	1.50	1.52	1.54	115	113	118
Acetylcholine chloride[b]	1.38	1.45	1.47	1.49	115	111	119
Carbamoylcholine bromide[c]	1.34	1.45	1.55	1.50	111	101	114
α-Methylacetylcholine iodide "A"[d]	1.30	1.46	1.45	1.52	122	109	111
α-Methylacetylcholine iodide "B"[d]	1.45	1.40	1.59	1.54	120	101	113
β-Methylacetylcholine iodide[e]	1.25	1.54	1.43	1.59	126	107	114
erythro-Dimethylacetylcholine iodide[f]	1.35	1.46	1.46	1.55	119	106	113
threo-Dimethylacetylcholine iodide[f]	1.32	1.55	1.57	1.50	114	103	108
Muscarine iodide[g]	1.47	1.47	1.53	1.48	109	110	113
(+)-*trans*-ACTM[h]	1.38	1.44	1.49	1.52	116	112	119
"F-2268"[i]	1.49	1.36	1.35	1.54	127	103	127
Choline chloride[j]		1.39	1.56	1.59		112	112
Glycerophosphorylcholine[k]		1.43	1.52	1.50		112	115
Average	1.368	1.454	1.499	1.528	117.6	107.7	115.1
Standard deviation	0.075	0.055	0.067	0.035	5.8	4.5	4.8

[a] Reference 17. [b] Reference 18. [c] Y. Barrans and M. J. Clastre, *C. R. Hebd. Seances Acad. Sci., Ser. C*, **270**, 306 (1970). [d] C. Chothia and P. Pauling, *Chem. Commun.*, 746 (1969). [e] Reference 19. [f] E. Shefter, P. Sackman, W. F. Stephen, and E. E. Smissman, *J. Pharm. Sci.*, 59, 1118 (1970). [g] F. Jellinek, *Acta Crystallogr.*, **10**, 277 (1957). [h] C. Chothia and P. Pauling, *Nature (London)*, **226**, 541 (1970). [i] P. J. Pauling and T. J. Petcher, *J. Med. Chem.*, **14**, 3 (1971). [j] M. E. Senko and D. H. Templeton, *Acta Crystallogr.*, **13**, 281 (1960). [k] S. Abrahamsson and I. Pascher, *ibid.*, **21**, 79 (1966).

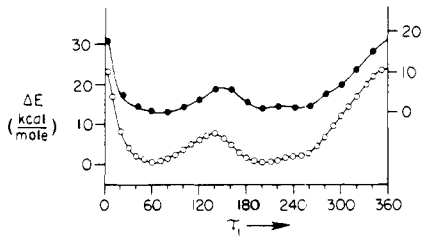

Figure 14. Comparison of empirical and INDO energies of β-methylacetylchlorine as a function of τ_1, with τ_2 fixed at 60°, using flexible geometries obtained from minimization of empirical energy with constrained dihedral angles: (○) empirical energy (left-hand scale); (●) INDO energy (right-hand scale).

14, in which the zero of energy has been chosen differently for each curve; the relative placement of curves is only for convenience. Both figures show variation of the energy as a function of τ_1, with τ_2 kept fixed at 60°. The geometries used in Figure 13 were generated from the rigid iodide crystal geometry, while Figure 14 was obtained using the flexible geometries found while preparing the flexible-geometry map for β-methylacetylcholine. Thus the first case is one in which significant nonbonded repulsions are present (at the ends of the slice) while in the second case nonbonded repulsions have been substantially removed by allowing the geometry to relax in accord with the potential function of eq 1. Figure 13 shows that the INDO minima are much closer to the steep repulsion barriers; this type of behavior has been discussed by Froimowitz and Gans.[6] Their Table VI shows the appreciable number of short interatomic distances present in local-minimum conformations found by the INDO method; clearly the same phenomenon is at work in Figure 13.

The striking parallel between empirical and INDO energy curves across the entire slice in Figure 14 suggests that the portions of the intramolecular potential *other* than nonbonded interactions behave very similarly in the two energy formulations. It also suggests that if flexible-geometry calculations were carried out using INDO or another semiempirical method, the results would be similar to those presented here. The essential point is that with the large nonbonded contributions removed by means of a flexible geometry, the remaining portion of eq 1 gives a molecular potential very similar to that obtained by the INDO formulation.

VI. Conclusions

Empirical energy-function calculations have been performed to investigate the effects of structural flexibility on potential energy surfaces. It is clear from the results that flexibility greatly expands the conformational space accessible to a molecule, especially if the rigid-geometry map indicates significant steric hindrance. It appears, nevertheless, that the general positions of energy minima on the surface are not strongly dependent on including structural flexibility in the calculation. What varies most are the energy barriers, which arise primarily from short-range nonbonded repulsions.

From the present work it can be concluded that some caution is required in interpreting available rigid-geometry maps. Considering both the increased conformational space available when geometric flexibility is present, and the possibility that a receptor may provide some energy for reorientation of its substrate, it is evident that considerable care is required in basing conclusions concerning the active conformation of a molecule solely on a rigid-geometry map.

Acknowledgment. We wish to acknowledge helpful discussions and assistance from Dr. A. Warshel in modifying the empirical energy program for the present application. Also, we are grateful for a contribution of time on the SDS Sigma 7 computer of the Department of Physics, Harvard University. B.G. acknowledges support from National Science Foundation Training Grants.

Appendix

X-Ray Structural Parameters of Cholineric Molecules. Table VI shows X-ray structural parameters for the C6–O1–C5–C4–N^+ portion of several acetylcholine-related molecules, along with their averages and standard deviations. The range of values and differences among very similar compounds indicates that no one structure can be regarded as the obvious choice for rigid-geometry mapping. For example, the two structures for acetylcholine (bromide

and chloride) and the two structures for α-methylacetylcholine iodide contain bond length and bond angle differences which are large enough to affect the rigid-geometry maps (see section IV). However, it is not clear because of the crudeness of some of the X-ray determinations whether the surprisingly large differences found in some of the cases are actually correct. It seems desirable, therefore, that more precise data be obtained for these and similar molecules. If the differences do turn out to be real, it is clear that straightforward averaging to obtain a "standard" structure, which neglects particulars of chain substitution, crystal packing, and other possible chemical differences is not valid and further investigation of these interactions will be required.

References and Notes

(1) Supported in part by the National Science Foundation (U.S.A.), the National Institutes of Health (U.S.A.), and Centre National de la Recherche Scientifique (France).
(2) Address correspondence to this author at Harvard University.
(3) L. B. Kier, "Molecular Orbital Theory in Drug Research", Academic Press, New York, N.Y., 1971; B. Pullman and B. Maigret, "Proceedings of the Fifth Jerusalem Symposium on the Conformation of Biological Molecules and Polymers", Academic Press, New York, N.Y., 1973.
(4) (a) L. B. Kier, *Mol. Pharmacol.*, **3**, 487 (1967); (b) A. M. Liquori, A. Damiani, and J. L. DeCoen, *J. Mol. Biol.*, **33**, 445 (1968); (c) B. Pullman, P. Courriere, and J. B. Coubeils, *Mol. Pharmacol.*, **7**, 397 (1971).
(5) D. Ajo, M. Bossa, A. Damiani, R. Fidenzi, S. Gigli, L. Lanzi, and A. Lapiccirella, *J. Theor. Biol.*, **34**, 15 (1972).
(6) M. Froimowitz and P. J. Gans, *J. Am. Chem. Soc.*, **94**, 8020 (1972).
(7) D. W. Genson and R. E. Christoffersen, *J. Am. Chem. Soc.*, **95**, 362 (1973).
(8) D. L. Beveridge and R. J. Radna, *J. Am. Chem. Soc.*, **93**, 3759 (1971).
(9) R. J. Radna, D. L. Beveridge, and A. L. Bender, *J. Am. Chem. Soc.*, **95**, 3831 (1973).
(10) D. Ajo, M. Bossa, R. Fidenzi, S. Gigli, and G. Jeronimidis, *Theor. Chim. Acta*, **30**, 275 (1973).
(11) B. Pullman and P. Courriere, *Mol. Pharmacol.*, **9**, 612 (1972).
(12) B. Pullman and P. Courriere, *Theor. Chim. Acta*, **31**, 19 (1973).
(13) G. N. J. Port and A. Pullman, *J. Am. Chem. Soc.*, **95**, 4059 (1973).
(14) S. Lifson and A. Warshel, *J. Chem. Phys.*, **49**, 5116 (1968); A. Warshel and S. Lifson, *ibid.*, **53**, 582 (1970).
(15) A. Warshel, M. Levitt, and S. Lifson, *J. Mol. Spectrosc.*, **33**, 84 (1970); S. Karplus and S. Lifson, *Biopolymers*, **10**, 1973 (1971).
(16) A. Warshel and M. Karplus, *J. Am. Chem. Soc.*, **94**, 5612 (1972).
(17) F. G. Canepa, P. J. Pauling, and H. Sörum, *Nature (London)*, **210**, 907 (1966).
(18) J. K. Herdklotz and R. L. Sass, *Biochem. Biophys. Res. Commun.*, **40**, 583 (1970).
(19) C. H. Chothia and P. J. Pauling, *Chem. Commun.*, 626 (1969).
(20) J.-P. Behr and J.-M. Lehn, *Biochem. Biophys. Res. Commun.*, **49**, 1573 (1972).
(21) D. Lichtenberg, P. A. Kroon, and S. I. Chan, *J. Am. Chem. Soc.*, **96**, 5934 (1974).
(22) D. L. Beveridge, M. M. Kelly, and R. J. Radna, *J. Am. Chem. Soc.*, **96**, 3769 (1974).
(23) F. K. Winkler and J. D. Dunitz, *J. Mol. Biol.*, **59**, 169 (1971).

Equilibrium Acidities of Carbon Acids. VI. Establishment of an Absolute Scale of Acidities in Dimethyl Sulfoxide Solution[1]

Walter S. Matthews,[2] Joseph E. Bares, John E. Bartmess, F. G. Bordwell,* Frederick J. Cornforth, George E. Drucker, Zafra Margolin, Robert J. McCallum, Gregory J. McCollum, and Noel R. Vanier

Contribution from the Department of Chemistry, Northwestern University, Evanston, Illinois 60201.

Received April 2, 1975

Abstract: An accurate spectrophotometric method of determining relative equilibrium acidities of carbon acids in DMSO has been developed. The pK scale in DMSO has been anchored by comparisons of values obtained by the spectrophotometric method with those obtained potentiometrically in the 8 to 11 pK range. As a result, the pK of fluorene, formerly arbitrarily taken as 20.5, has been raised to an absolute value of 22.6. The pK's of other carbon acids previously reported, including nitromethane, acetophenone, acetone, phenylacetylene, dimethyl sulfone, acetonitrile, and the corresponding indicator pK's must also be raised. The pK's have been found to be correlated with heats of deprotonation in DMSO by potassium dimsyl, and evidence is presented to show that pK measurements in DMSO are free from ion association effects. Data are presented which indicate a pK of 35.1 for DMSO. In the methane carbon acids, CH_3EWG, the order of acidities is $NO_2 \gg CH_3CO >$ CN, CH_3SO_2. The differences amount to 12.2 and 6.8 kcal/mol, respectively, which are believed to be of a comparable magnitude to gas-phase substituent effects. Carbon acids wherein the charge on the anion resides mainly on oxygen, such as ketones and nitroalkanes, are found to be weaker acids in DMSO than in water by 5.5 to 9.6 pK units. On the other hand, carbon acids wherein the charge on the anion is delocalized over a large hydrocarbon matrix, such as in the anion derived from 9-cyanofluorene, are stronger acids in DMSO than in water. Factors that may contribute to this reversal are discussed. The scale of pK's for 9-substituted fluorenes in DMSO is shown to be expanded when compared to the earlier pK scale determined by the H_- method. A rationale is presented. The apparent relative acidities of fluorenes and phenylacetylene differ by 6 and 11 pK units, respectively, for cyclohexylamine (CHA) vs. DMSO solvents and benzene vs. DMSO solvents. Similarly, in benzene, acetophenone is a stronger acid than fluorene by ca. 6 pK units, whereas in DMSO acetophenone is a weaker acid by 3.2 pK units. These differences result from ion association effects that occur in solvents of low dielectric constant (benzene, ether, CHA, etc.) causing relative acidities to be dependent on the reference base, as well as the solvent. This is not true in strongly dissociating solvents of high dielectric constant, such as DMSO. A list of 13 indicators covering the pK range 8.3 to 30.6 in DMSO is presented.

Equilibrium acidities of weak (i.e., p$K \geq 15$) carbon acids have been measured by a variety of methods[3] in a variety of solvents including ether,[4a] benzene,[4b] diglyme,[5] cyclohexylamine (CHA),[6] mixtures of dimethyl sulfoxide (DMSO) with ethanol, methanol, or water,[7,8,9] and pure DMSO.[10] We have chosen DMSO for our studies because it allows accurate measurements to be made spectrophotometrically for many different types of carbon acids over a wide range of pK (ca. 30 pK units) with apparently little or no interference from ion association effects.[1] Furthermore,